RNA (1997), 3:961-973. Cambridge University Press. Printed in the USA.

Kinetics of hairpin ribozyme cleavage in yeast

CHRISTINE P. DONAHUE and MARTHA J. FEDOR

Department of Biochemistry and Molecular Biology, University of Massachusetts Medical Center, Worcester, Massachusetts 01655-0103, USA

ABSTRACT

Hairpin ribozymes catalyze a self-cleavage reaction that provides a simple model for quantitative analyses of intracellular mechanisms of RNA catalysis. Decay rates of chimeric mRNAs containing self-cleaving ribozymes give a direct measure of intracellular cleavage kinetics in yeast. Intracellular ribozyme-mediated cleavage occurs at similar rates and shows similar inhibition by ribozyme mutations as ribozyme-mediated reactions in vitro, but only when ribozymes are located in a favorable mRNA sequence context. The impact of cleavage on mRNA abundance is shown to depend directly on intrinsic mRNA stability. Surprisingly, cleavage products are no more labile than uncleaved mRNAs despite the loss of terminal cap structures or poly (A).

Keywords: antisense RNA; kinetic analysis; mRNA degradation; poly A removal; hairpin ribozyme; RNA stability

INTRODUCTION

Kinetic and thermodynamic analyses have provided crucial insights into the mechanistic details that determine the efficiency and specificity of RNA-catalyzed reactions in vitro. Despite the recent focus on RNA-catalyzed reactions in translation (Noller et al., 1992), in precursor mRNA splicing (Madhani & Guthrie, 1992), and on gene inactivation through antisense ribozyme-mediated RNA cleavage in vivo, it remains unclear how mechanisms defined for RNA catalysts in vitro relate to RNA-mediated reactions in cells. Antisense ribozyme cleavage activity in vitro correlates poorly with gene inactivation in vivo (Crisell et al., 1993; Homann et al., 1994). Self-splicing of pre-rRNA is not only much faster in vivo than in vitro, but a mutation that eliminates detectable self-splicing in vitro is compensated substantially in vivo (Brehm & Cech, 1983; Zhang et al., 1995). Thus, the available evidence points to fundamental differences between in vivo and in vitro mechanisms of RNA catalysis.

In vivo, RNA-binding proteins may influence catalytic RNA structures by "capturing" active conformations or by destabilizing inactive ones (Mohr et al., 1992; Tsuchihashi et al., 1993; Bertrand & Rossi, 1994; Coetzee et al., 1994; Weeks & Cech, 1995) or even participate directly in catalytic chemistry. Differences between RNA-catalyzed reactions in vivo and in vitro also could arise from an ionic environment that is more or less favorable for ribozyme assembly and catalysis because both RNA folding and catalytic chemistry depend strongly on the identity and concentrations of ions (Grosshans & Cech, 1989; Celander & Cech, 1991; Smith et al., 1992; Pan et al., 1993; Piccirilli et al., 1993; Chowrira et al., 1993; Zarrinkar & Williamson, 1994; Pan, 1995).

To begin to understand how the mechanisms of RNA catalysis elucidated through in vitro studies relate to the behavior of RNA enzymes inside cells, we have undertaken a quantitative analysis of a simple RNA-catalyzed reaction in yeast. The hairpin ribozyme catalyzes reversible self-cleavage to process intermediates in rolling circle replication of plant satellite RNAs (Keese & Symons, 1987). Together with the hammerhead, axehead, and *Neurospora* VS catalytic RNAs, the hairpin belongs to the family of small RNA enzymes that cleave phosphodiesters to generate 5′ hydroxyl and 2′,3′-cyclic phosphate termini (reviewed in Symons, 1992; Long & Uhlenbeck, 1993). A hairpin secondary structure model consisting of two pairs of helix-loop-helix segments has been confirmed experimentally and the two segments appear to interact within a noncoaxial tertiary structure (reviewed in Burke et al., 1996; Fig. 1A).

Although the hairpin ribozyme assembles from sequences within one RNA in nature, the ribozyme can be designed to recognize and cleave separate RNA substrates (Hampel & Tritz, 1989). Rate and equilibrium constants have been determined for individual steps of intermolecular cleavage and ligation reactions

Reprint requests to: Martha Fedor, The Skaggs Institute for Chemical Biology, The Scripps Research Institute, 10550 North Torrey Pines Road, La Jolla, California 92037, USA; e-mail: mfedor@scripps.edu.

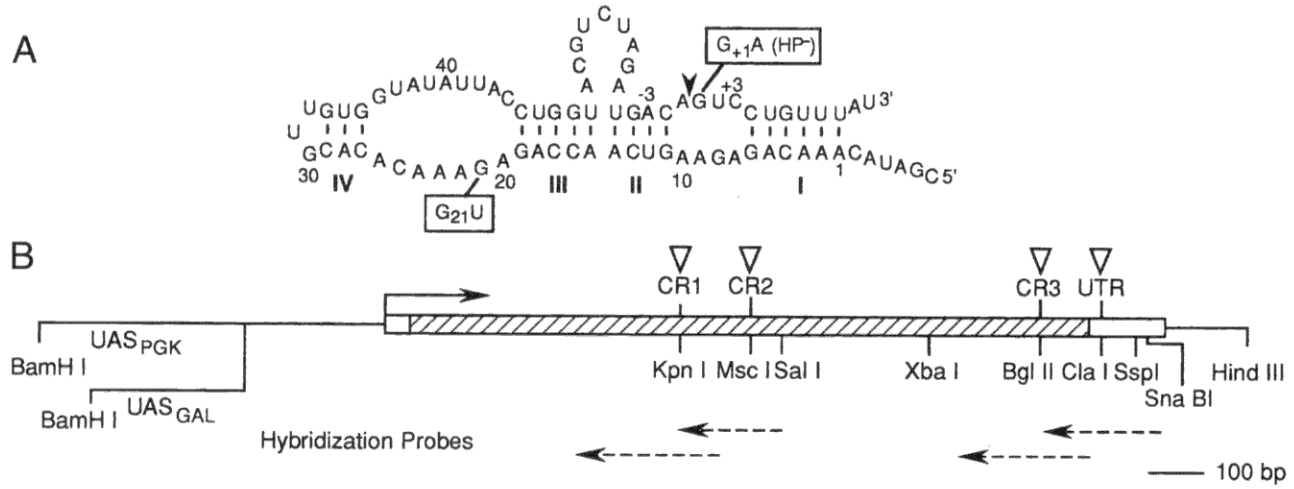

FIGURE 1. Hairpin ribozymes and chimeric *PGK1* genes. **A:** Hairpin ribozyme sequences and secondary structure model. The self-cleaving hairpin ribozyme has the same sequence as the hairpin domain of tobacco ringspot virus satellite RNA with linkers between helices II and III and at the base of helix IV replacing satellite RNA sequences that are not required for catalysis. Base paired helices I, II, III, and IV are indicated. Arrow indicates the reactive phosphodiester. Mutations that eliminate ($G_{+1}A$) or reduce ($G_{21}U$) catalytic activity are boxed. **B:** Chimeric *PGK1* genes and RNAs. Oligonucleotides encoding hairpin ribozymes were inserted into the 3′ untranslated region (open rectangle, UTR) or the coding region (hatched rectangle, CR1, CR2, and CR3) of the yeast *PGK1* gene. Chimeric mRNAs were expressed from the natural *PGK1* promoter or under the control of GAL1-10 regulatory sequences. The mRNA transcription start site is indicated by a solid arrow. ^{32}P-labeled transcripts (dashed arrows) were used as probes in hybridization-RNase protection assays. Transcripts with the opposite polarity were used to measure self-cleavage kinetics in vitro.

(Hegg & Fedor, 1995). The hairpin ribozyme imposes few constraints on substrate sequences beyond the ability to form base paired helices with the ribozyme. Consequently, hairpin ribozymes can be engineered to cleave virtually any target RNA through simple adherence to Watson–Crick base pairing rules. Hairpin ribozymes directed against HIV-1 sequences protect primary human lymphocytes from infection in culture and have entered clinical trials (Welch et al., 1996).

Hairpin ribozymes were expressed in yeast as self-cleaving mRNAs. Differences between decay rates of chimeric mRNAs that contain functional or inactive hairpin ribozymes reflect intracellular cleavage kinetics directly. In favorable mRNA sequence contexts in vivo, ribozymes self-cleave at rates similar to self-cleavage rates measured in vitro. A ribozyme mutation that slows cleavage in vitro also slows intracellular cleavage by a similar amount. Thus, the reaction pathway and the rate-determining step or steps for hairpin ribozyme-mediated cleavage are fundamentally the same in vitro and in vivo. Ribozymes located in unfavorable mRNA sequence contexts react poorly in vivo, evidence that features of native mRNA structure or activity can impede ribozyme assembly. The impact of self-cleavage on mRNA abundance reflects the ratio of self-cleavage and intrinsic mRNA turnover rates, demonstrating that antisense ribozymes will be most effective when directed against stable RNA targets. Finally, we show that the products of intracellular cleavage lacking terminal cap structures and poly (A) degrade no faster than uncleaved mRNAs.

RESULTS

Monitoring hairpin ribozyme-mediated cleavage in yeast

To examine intracellular catalysis directly, without interference from transport or binding steps that might limit ribozyme cleavage of separate RNA substrates, hairpin ribozymes were expressed in yeast as self-cleaving mRNAs (Fig. 1). The ribozyme sequence is derived from the self-cleaving domain in the negative strand of the satellite RNA of tobacco ringspot virus (Buzayan et al., 1986; Feldstein et al., 1989; Hampel & Tritz, 1989).

The hairpin ribozyme sequence (HP) was inserted into a plasmid-born *PGK1* gene, a yeast gene chosen for the abundance and slow turnover of its mRNA that provide a sensitive gauge for any ribozyme cleavage-mediated acceleration of mRNA decay (Herrick et al., 1990; Peltz & Jacobson, 1993). Chimeric mRNA containing a self-cleaving hairpin ribozyme (HP mRNA) was compared to the same mRNA containing a $G_{+1}A$ point mutation in the hairpin sequence (HP^- mRNA) that eliminates catalytic activity (Chowrira et al., 1991) to distinguish effects of self-cleavage from effects of insertion of ribozyme sequences on mRNA stability.

It was first important to ensure that any observed cleavage occurs in vivo and not during isolation of yeast RNA. To monitor self-cleavage during RNA isolation, uncleaved ^{32}P-labeled chimeric HP RNA was purified from in vitro transcription reactions, combined with yeast, and subjected to conventional RNA

extraction procedures (Köhrer & Domdey, 1991; Kaiser et al., 1994). Although efficient catalysis requires metal cations that should be chelated by extraction buffers (Hampel & Tritz, 1989; Chowrira et al., 1993), almost 20% of the added ^{32}P RNA self-cleaved during extraction or during storage in water (Fig. 2). Cleavage extents approached 50% when RNA samples were frozen and thawed repeatedly (not shown). Evidently, even slow cleavage rates allow significant product accumulation over the time required for RNA analysis. When RNA is extracted and stored in buffer at pH 5, however, the added ^{32}P HP RNA remains intact. To ensure that any cleavage products detected in yeast RNA arise only from intracellular cleavage, yeast RNA was purified and stored at low pH for all further experiments.

The hairpin ribozyme self-cleaves in yeast

We used hybridization-RNAse protection assays to analyze products of intracellular cleavage. RNA from yeast carrying a chimeric *PGK1* gene with a ribozyme insertion in the 3′ untranslated region (HP mRNA) was annealed with a ^{32}P-labeled transcript of *PGK1* sequences containing an insertion complementary to the ribozyme (HP^{anti} transcript, Fig. 3A). Samples were digested with RNAse to remove unhybridized sequences and protected fragments were fractionated on denaturing gels. Uncleaved chimeric RNA and 5′ cleavage product were purified from in vitro transcription reactions to provide markers for comparison. Uncleaved chimeric RNA was either maintained in 10 mM $NaCO_2CH_3$, 1 mM EDTA, pH 5, to prevent cleavage, or diluted into 50 mM Tris-Cl, 10 mM $MgCl_2$, 0.1 mM EDTA, pH 7.5, and allowed to react to completion.

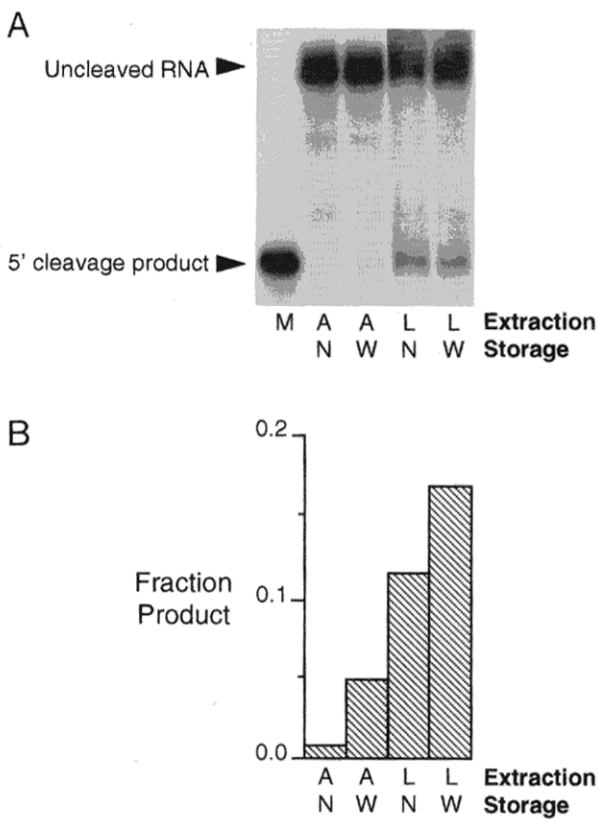

FIGURE 2. Self-cleavage during preparation of yeast RNA. RNA was extracted from yeast using acidic phenol (A) or LiCl (L) and stored in 10 mM $NaCO_2CH_3$, 1 mM EDTA, pH 5, buffer (N) or water (W). ^{32}P-labeled ribozyme transcripts were combined with yeast to monitor self-cleavage during RNA extraction. ^{32}P-labeled uncleaved chimeric RNA or 5′ cleavage products, either purified from in vitro transcription reactions or generated by self-cleavage during yeast RNA purification, were fractionated on denaturing gels (**A**) and quantitated by radioanalytic scanning (**B**).

Chimeric yeast mRNA and chimeric RNA transcripts allowed to undergo self-cleavage in vitro generated virtually the same fragments with 70% of yeast HP mRNA sequences co-migrating with the 5′ cleavage product marker (Fig. 3B,C). An 11-nt fragment arising from the 3′ cleavage product would have been too small to detect. Uncleaved HP RNA that was maintained at low pH to prevent self-cleavage remained virtually intact under assay conditions, further evidence that cleavage products detected in yeast mRNA arose from intracellular cleavage and not during the analysis (Fig. 3B,C). Thus, chimeric HP mRNA self-cleaves at the appropriate site in yeast.

Larger hybridization probes that span the ribozyme insertion sites (Fig. 1B; Table 1) monitor mRNAs expressed from genomic *PGK1* mRNA and chimeric mRNAs in the same assay to allow comparisons of intracellular RNA abundance. As expected, HP$^-$ mRNA, containing a $G_{+1}A$ mutation that eliminates hairpin cleavage in vitro, produced no cleavage products (Fig. 3D). The similar abundance of HP$^-$ and genomic mRNAs indicates that ribozyme sequences had little effect on transcription or on mRNA stability in the absence of cleavage (Fig. 3D,E). Consistent with appearance of 70% of HP mRNA sequences as cleavage products, uncleaved HP mRNA levels were nearly 70% lower than HP$^-$ and genomic mRNA levels. The total amount of HP mRNA, including uncleaved mRNA and cleavage products, however, was similar to the amount of HP$^-$ and genomic mRNAs. If cleavage products were significantly less stable than uncleaved mRNAs, the total amount of HP mRNA sequences would have decreased. Quantitative analysis of cleavage product stability is presented below. Furthermore, the 5′ cleavage product was nearly threefold more abundant than the 3′ cleavage product. Because both products would arise in equal amounts through in vitro cleavage, this difference between 5′ and 3′ product levels confirms that products arose in vivo.

Hairpin ribozymes cleave at similar rates in vivo and in vitro

The steady-state concentration of an mRNA reflects the balance between rates of transcription and decay.

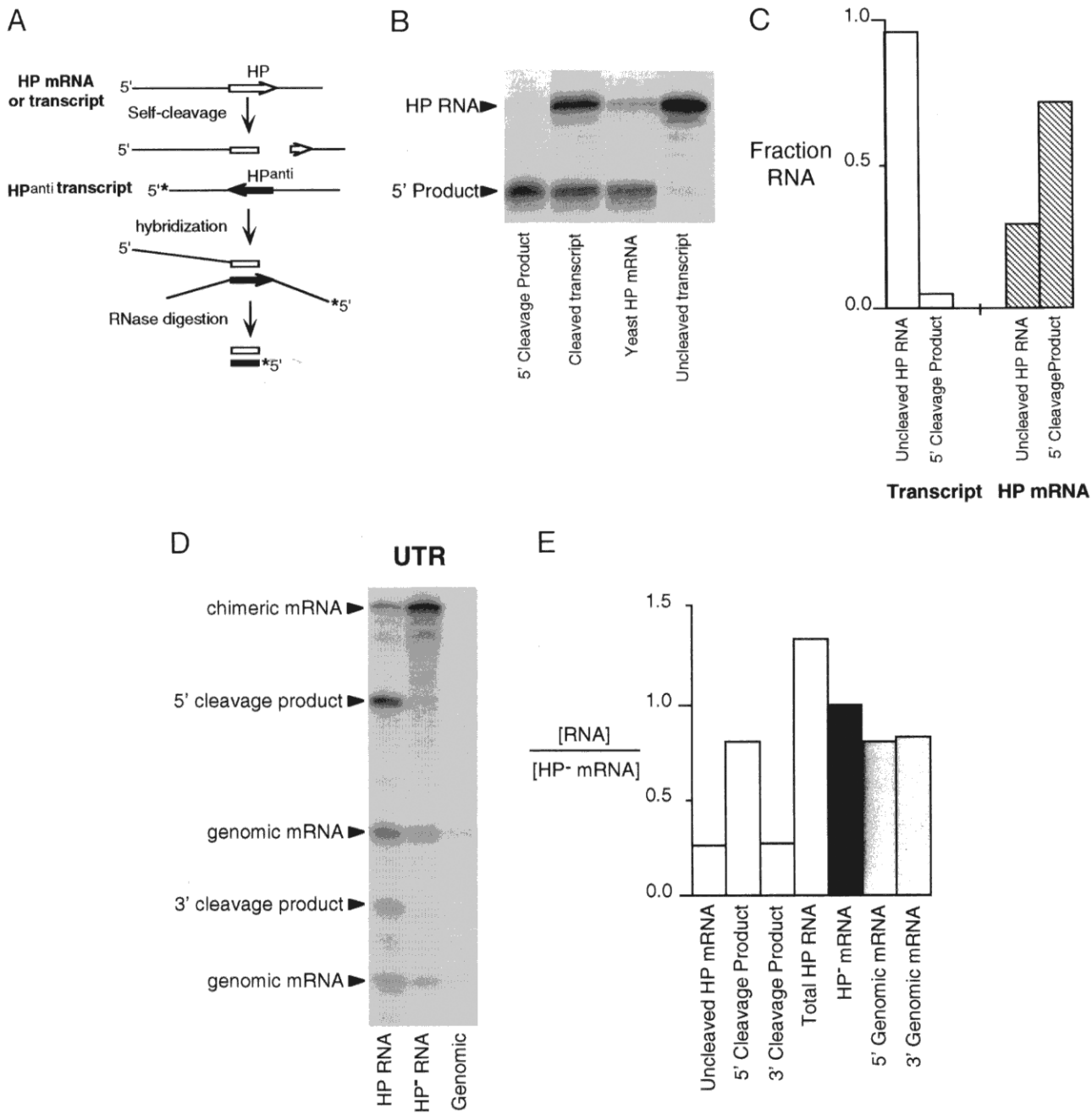

FIGURE 3. Hairpin ribozyme self-cleavage in vivo. **A:** Comparison of intracellular and in vitro self-cleavage products using hybridization-RNase protection assays. RNA from yeast carrying a chimeric *PGK1* gene with a ribozyme insertion in the 3′ untranslated region (HP mRNA, open arrow) were annealed with an [α-^{32}P]-labeled transcript of *PGK1* sequences containing an insertion complementary to the ribozyme (*HP^{anti} transcript, filled arrow). RNAs were treated with RNase to remove unhybridized PGK1 sequences and protected fragments were fractionated on denaturing gels. Chimeric RNAs transcribed in vitro were analyzed in parallel reactions to provide cleavage product markers. **B:** The same fragments are produced by intracellular and in vitro self-cleavage. Yeast HP mRNA and chimeric RNA transcripts allowed to undergo cleavage in vitro (cleaved transcript) produce the same fragments that co-migrate with 5′ cleavage product purified from an in vitro transcription reaction and with uncleaved HP RNA purified from an in vitro transcription reaction and maintained in 10 mM $NaCO_2CH_3$, 1 mM EDTA, pH 5 (uncleaved transcript). **C:** Relative abundance of uncleaved HP mRNA and 5′ cleavage product detected in assays of B. **D:** Arrows mark fragments corresponding to uncleaved chimeric mRNA, cleavage products, and genomic *PGK1* mRNA sequences detected in yeast carrying functional (HP) or inactive (HP$^-$) hairpin ribozymes in the 3′ untranslated region of plasmid-born *PGK1* genes, or carrying only genomic *PGK1*. Fragments were detected using the hybridization probe complementary to the 3′UTR ribozyme insertion site shown in Figure 1B. **E:** Abundance of HP mRNA and cleavage products (open) and genomic *PGK1* mRNA sequences 5′ and 3′ of the ribozyme insertion site (shaded) are shown relative to the amount of HP$^-$ mRNA (filled).

TABLE 1. Analysis of intracellular cleavage products.

Insertion site	Cleavage product	Fragment expected[a] (nucleotides)	Fragment observed[b] (nucleotides)
CR1	5′	270	284
	3′	90	101
CR2	5′	207	226
	3′	86	88
CR3	5′	203	220
	3′	96	97
UTR	5′	181	200
	3′	102	102

[a]Sizes of fragments expected for products of intracellular self-cleavage of chimeric mRNAs using hybridization-RNAse protection assays with the hybridization probes indicated in Figure 1.

[b]Sizes of fragments determined in hybridization-RNAse protection assays shown in Figures 3D and 6A were calculated from electrophoretic mobility by comparison with fragments produced by uncleaved chimeric mRNA and genomic PGK1 mRNA fragments.

Because most HP mRNA is cleaved at steady state, the time required for intracellular cleavage is less than the lifetime of the mRNA. The cleavage rate can be measured directly from the effect of self-cleavage on HP mRNA turnover. HP mRNA decays both through self-cleavage and through the pathway responsible for normal mRNA degradation, whereas HP^- mRNA decays only through the endogenous degradation pathway (Fig. 4A). Consequently, self-cleavage accelerates decay of HP mRNA relative to HP^- mRNA by an amount corresponding to the intracellular cleavage rate.

To obtain a population of HP mRNA that had not yet cleaved, a burst of transcription was induced from chimeric *PGK1* genes fused to a galactose-inducible promoter. After further transcription was inhibited by addition of glucose to growth media, we monitored the disappearance of uncleaved HP mRNA over time (Fig. 4B). The distinct lag in the decay of 5′ cleavage product corresponds to the phase in which product degradation is nearly balanced by self-cleavage of newly transcribed HP mRNA. The change in the proportion of uncleaved HP mRNA and 5′ cleavage product over the decay time course provides more strong evidence that self-cleavage occurred in vivo. Because RNAs were analyzed in parallel from yeast collected at different times, any cleavage that occurred in vitro would have reached the same extent in RNA from each time point.

A parallel pulse-chase experiment with HP^- mRNA gives the intrinsic rate of chimeric mRNA degradation through the normal mRNA turnover pathway. HP^- mRNA displayed a half life similar to that measured previously for genomic *PGK1* mRNA (Herrick et al., 1990), whereas HP mRNA disappeared almost three times faster (Fig. 4B, inset; Table 2). The difference between HP and HP^- mRNA decay rates gives a value of 0.046 min^{-1} for the rate of intracellular cleavage (Table 2).

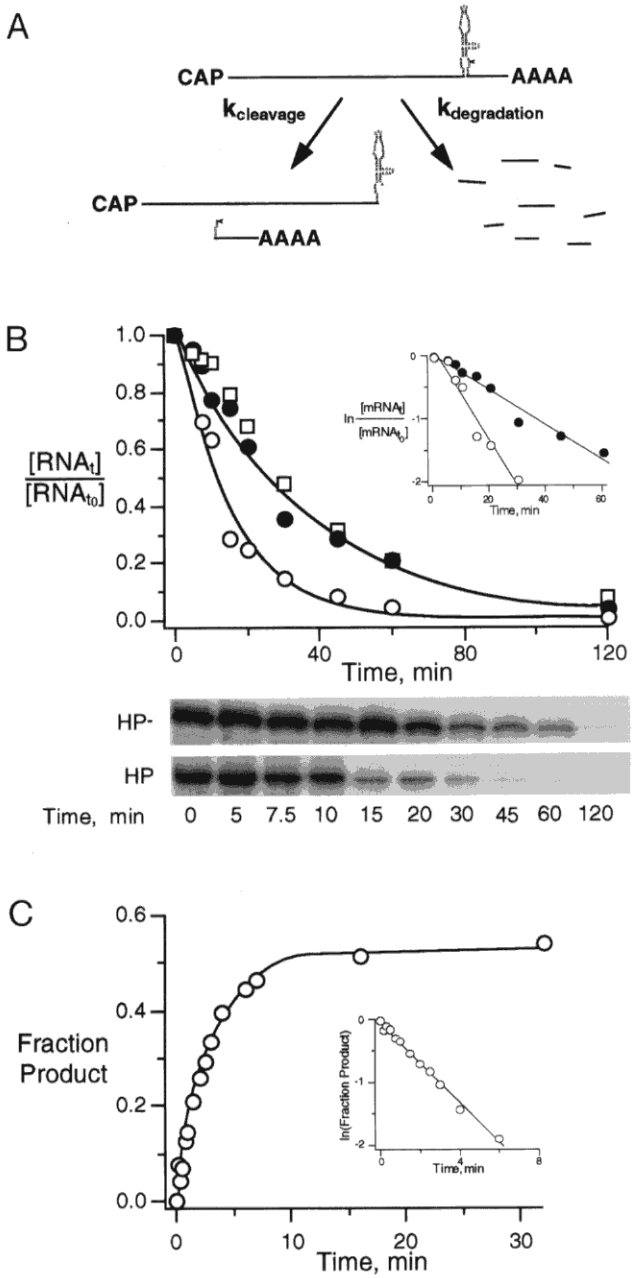

FIGURE 4. Self-cleavage kinetics of a hairpin ribozyme in the 3′UTR of *PGK1* mRNA. **A:** HP mRNA decays both through self-cleavage ($k_{cleavage}$) and through the pathway responsible for normal mRNA degradation ($k_{degradation}$), whereas HP^- mRNA decays only through the normal mRNA degradation pathway. Self-cleavage accelerates decay of HP mRNA relative to HP^- mRNA by an amount corresponding to the intracellular cleavage rate. **B:** Intracellular self-cleavage kinetics. Uncleaved HP mRNA (open circles), 5′ cleavage product (open squares), and HP^- mRNA (filled circles) were quantitated at various times after a burst of transcription using hybridization-RNase protection assays. Chimeric mRNA decay rates were determined from fits to $([RNA_t]/[RNA_{t0}]) = e^{-kt}$ and $\ln([RNA_t]/[RNA_{t0}]) = -kt$ (inset). The difference between the HP mRNA decay rate of 0.072 min^{-1} and the HP^- mRNA decay rate of 0.026 min^{-1} gives an intracellular self-cleavage rate of 0.046 min^{-1}. Panels show fragments corresponding to uncleaved mRNA throughout the time course. **C:** In vitro self-cleavage kinetics. Uncleaved ^{32}P-labeled chimeric HP RNA transcripts were eluted from a denaturing gel and diluted into 50 mM Tris-Cl, 10 mM $MgCl_2$, 0.1 mM EDTA, pH 7.5, at 24 °C to initiate self-cleavage. Lines represent fits calculated to fraction product $= e^{-kt}$ and ln(fraction product) $= -kt$ (inset), giving a value of 0.33 min^{-1} for the rate of self-cleavage.

TABLE 2. Intracellular rates of hairpin ribozyme-mediated cleavage.

Insertion site	k_{decay}[a] (per min) HP (wild type)	k_{decay}[a] (per min) HP^{G21U} (impaired)	k_{decay}[a] (per min) HP^- (inactive)	$k_{cleavage}$[b] (per min)	[Chimeric mRNA]/[genomic PGK1 mRNA][d] HP (wild type)	[Chimeric mRNA]/[genomic PGK1 mRNA][d] HP^{G21U} (impaired)	[Chimeric mRNA]/[genomic PGK1 mRNA][d] HP^- (inactive)	$\frac{[HP]}{[HP^-]}$[f]	$k_{cleavage}$[g] (per min)
UTR	0.072 ± 0.02		0.026 ± 0.003	0.046	0.33 ± 0.3[e]		1.24 ± 0.73	0.26	0.071
UTR		0.038 ± 0.002	0.026 ± 0.003	0.012		0.84 ± 0.56		0.67	0.012
CR1	0.073 ± 0.007		0.064 ± 0.005	0.0097	0.48 ± 0.03		0.73 ± 0.02	0.66	0.033
CR2	0.059 ± 0.004		0.058 ± 0.001	~0.015[c]	0.38 ± 0.15		0.37 ± 0.21	1.0	~0.015[c]
CR3	0.091 ± 0.01		0.040 ± 0.002	0.050	0.34 ± 0.06		0.91 ± 0.06	0.38	0.066

[a]Mean and range of values obtained in two or more measurements of intracellular chimeric mRNA decay rates.

[b]Calculated from $k_{cleavage} = k_{decay} - k_{degradation}$ using the difference in mean intracellular decay rates between HP and HP^- mRNA and assuming that k_{decay} for HP^- mRNA is $k_{degradation}$ and that k_{decay} for HP mRNA is the sum of $k_{degradation}$ and $k_{cleavage}$, as described in the text.

[c]Self-cleavage rate estimated from $k_{cleavage} = k_{degradation}$ ([5′ product]/[HP mRNA]) using the mean value for the relative abundance of 5′ product and HP mRNA shown in Table 3 and assuming that $k_{cleavage}$ [HP mRNA] = $k_{degradation}$ [product] at steady state and that 5′ products of CR2 cleavage degrade at the same rate as 5′ products of CR1 and UTR cleavage.

[d]Mean and range of values for the abundance of chimeric mRNA relative to genomic PGK1 mRNA in three or more preparations of yeast RNA.

[e]Standard deviation of values obtained from eight experiments was 0.15.

[f]Ratio of mean values of HP and HP^- mRNA abundance.

[g]Calculated from $k_{cleavage} = k_{degradation}$ ([HP^- mRNA]/[HP mRNA]) − $k_{degradation}$ using mean values for $k_{degradation}$ and for the relative abundance of HP and HP^- mRNAs and assuming that [HP mRNA]/[HP^- mRNA] = $k_{degradation}/(k_{degradation} + k_{cleavage})$ at steady state, as described in the text.

Having determined the intrinsic rate of HP^- mRNA degradation, the intracellular cleavage rate also can be calculated from the relative abundance of uncleaved HP and HP^- mRNAs at steady state (Brehm & Cech, 1983). The amount of HP^- mRNA at steady state reflects the balance of transcription and degradation, or:

$$[HP^- \text{ mRNA}] = \frac{k_{transcription}}{k_{degradation}}.$$

The amount of HP mRNA is given by:

$$[\text{HP mRNA}] = \frac{k_{transcription}}{k_{degradation} + k_{cleavage}},$$

and the ratio of HP mRNA and HP^- mRNA levels by:

$$\frac{[\text{HP mRNA}]}{[HP^- \text{ mRNA}]} = \frac{k_{degradation}}{k_{degradation} + k_{cleavage}}.$$

The ratio of HP and HP^- mRNA abundance (Fig. 3E) combined with the rate measured for HP^- mRNA degradation (Fig. 4B) gives a value for $k_{cleavage}$ of 0.071 min^{-1}, in good agreement with the value of 0.046 min^{-1} determined directly from HP mRNA decay kinetics (Table 2). Thus, different calculations based on two sets of measurements give consistent values averaging 0.06 min^{-1} for the intracellular cleavage rate.

With a half-life of ~12 min, intracellular self-cleavage is only fivefold slower than self-cleavage of chimeric HP transcripts in vitro (Fig. 4C) or than cleavage rate constants measured for intermolecular reactions in vitro (Hegg & Fedor, 1995). Because intracellular self-cleavage is slower than the lifetime of most yeast mRNAs (Herrick et al., 1990), cleavage almost certainly occurs in the cytoplasm after most intracellular activities of the mRNA are complete.

Intracellular and in vitro hairpin ribozyme cleavage mechanisms are similar

The similarity of intracellular and in vitro cleavage rates suggests that the mechanism of hairpin ribozyme-mediated cleavage is the same in vivo and in vitro and that reaction rates are determined by the same step or steps in both environments. If catalysis is very rapid in vivo but assembly of a functional ribozyme is slow, however, similar cleavage rates still could reflect different limiting steps in intracellular and in vitro reaction pathways. If cleavage is limited by a similar step in cells and in vitro, however, each reaction will show the same response to modifications that accelerate or inhibit cleavage.

To test whether a ribozyme mutation that impairs catalytic activity in vitro has the same effect in cells, we measured self-cleavage rates for chimeric RNAs with a $G_{21}U$ mutation. This mutation slowed in vitro self-cleavage 12-fold (Fig. 5A). Unless intracellular cleavage is limited by a different step, HP^{G21U} mRNA also will self-cleave at a slower rate. The difference between HP^- and HP^{G21U} mRNA decay rates and the relative abundance of intact HP^{G21U} and HP^- mRNAs at steady state give the same values for $k_{cleavage}$ of 0.012 min^{-1}, a rate about fivefold slower than intracellular self-cleavage of HP mRNA (Fig. 5B,C; Table 2). Because the $G_{21}U$ mutation inhibits intracellular and in vitro cleavage by similar amounts, in vitro and intracellular reactions likely proceed through similar mechanisms and share similar rate-determining steps.

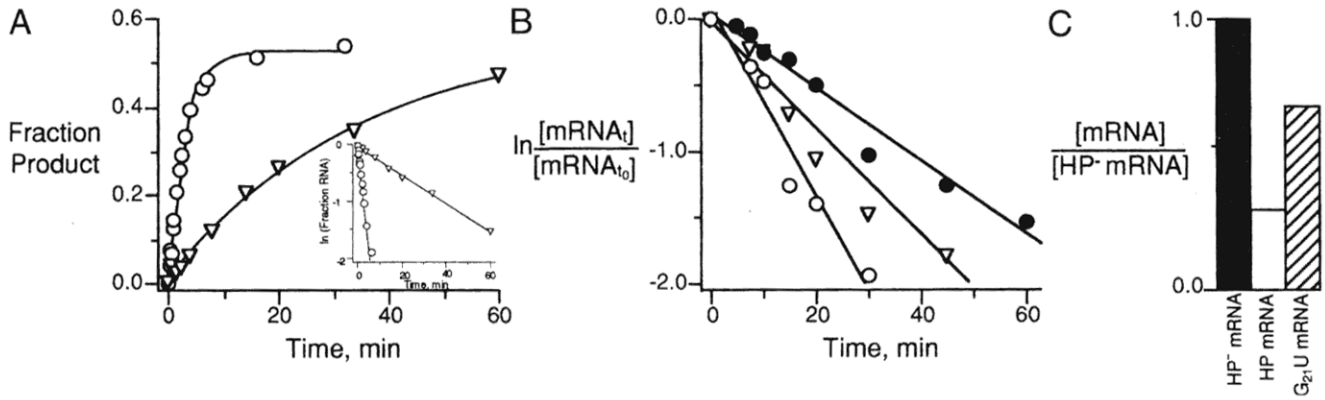

FIGURE 5. $G_{21}U$ mutation reduces self-cleavage rates in vitro and in vivo. **A:** Self-cleavage kinetics of $HP^{G_{21}U}$ RNA in vitro. Uncleaved ^{32}P-labeled chimeric HP (circle) and $HP^{G_{21}U}$ (triangle) transcripts were eluted from denaturing gels and diluted into reaction buffer to initiate self-cleavage. Lines represent fits calculated to fraction product = e^{-kt} and ln(fraction product) = $-kt$ (inset), giving cleavage rates of 0.33 min^{-1} and 0.027 min^{-1} for HP and $HP^{G_{21}U}$ RNAs, respectively. **B:** Self-cleavage kinetics of $HP^{G_{21}U}$ RNA in vivo. Uncleaved HP, $HP^{G_{21}U}$, and HP^- mRNAs were quantitated at various times after a burst of transcription using hybridization-RNAse protection assays. Decay rates of 0.072 min^{-1} for HP (open circle), 0.038 min^{-1} for $HP^{G_{21}U}$ (open triangle), and 0.026 min^{-1} for HP^- (filled circle) mRNAs were determined from fits to $\ln([RNA_t]/[RNA_{t0}]) = -kt$. The difference between $HP^{G_{21}U}$ and HP^- mRNA decay rates gives an intracellular self-cleavage rate of 0.012 min^{-1} for $HP^{G_{21}U}$ mRNA. **C:** Relative abundance of uncleaved HP^- mRNA (filled), HP mRNA (open), and $HP^{G_{21}U}$ mRNA (hatched) at steady state.

Hairpin self-cleavage efficiency varies with mRNA sequence context

Ribosome transit, differences in nucleoprotein structure between coding and noncoding mRNA sequences, or participation of mRNA sequences in stable secondary structures might influence ribozyme assembly. To learn whether hairpin ribozyme sequences located in different regions of mRNA display enhanced or diminished activity, self-cleaving ribozymes were inserted into three sites in *PGK1* coding sequences (Fig. 1B). In each case, the ribozyme insertion maintained an open reading frame. At steady-state, chimeric mRNA with a ribozyme in CR3 gives rise to about the same fraction of cleavage products as chimeric mRNA with a ribozyme in the UTR, whereas larger fractions of chimeric mRNA remain uncleaved when ribozymes are located in CR1 and CR2 (Fig. 6).

Apparent differences in cleavage efficiency instead could reflect differences in product stability if products of CR1 and CR2 cleavage degrade faster than products of UTR or CR3 cleavage. However, comparisons of chimeric mRNA abundance suggest that the context of the ribozyme insertion affects ribozyme activity and not product stability (Fig. 6B; Table 2). The total amount of all HP mRNAs, including uncleaved mRNA and cleavage products, was slightly higher than the amounts of corresponding HP^- mRNAs, evidence that products of CR1 and CR2 cleavage are no less stable than products of CR3 or UTR cleavage. Furthermore, with a ribozyme located at CR2, uncleaved HP and HP^- mRNAs levels were almost the same. Even if products of CR2 cleavage degrade rapidly, efficient cleavage would have depleted uncleaved HP mRNA.

Decay of HP^- mRNAs with CR1 and CR2 insertions was about twofold faster than decay of HP^- mRNA with a ribozyme in the UTR, indicating that inactive ribozyme insertions at these sites accelerated chimeric mRNA degradation somewhat (Fig. 7; Table 2). Faster intrinsic degradation rates reduce the impact of self-cleavage on uncleaved chimeric mRNA abundance (above). Therefore, variation in apparent cleavage extents results in part from differences in intrinsic degradation rates. Nonetheless, HP mRNA with a ribozyme in CR1 decays only slightly faster than corresponding HP^- mRNA, and chimeric mRNA with a ribozyme in CR2 displays no accelerated decay attributable to ribozyme-mediated cleavage. Cleavage-mediated acceleration of decay would have been detected easily if a ribozyme at CR2 self-cleaved at rates comparable to self-cleavage rates measured for CR3 and UTR insertions. Thus, native mRNA structure or activity can exert modest but clear effects on assembly of a functional ribozyme.

Chimeric RNAs also self-cleaved to different extents during transcription in vitro. However, variation in cleavage extents during in vitro transcription showed no correlation with self-cleavage efficiency in vivo, ranging from 35% self-cleavage for chimeric RNA with the CR3 ribozyme insertion that cleaved efficiently in yeast to 55% self-cleavage for chimeric RNA with a CR1 ribozyme insertion that cleaved poorly in yeast. Cleavage extents, but not cleavage rates, also varied in reactions initiated by diluting purified ribozyme transcripts into reaction buffer, but again showed no correlation with intracellular self-cleavage efficiency (data not shown). The propensity of some RNAs to adopt nonfunctional structures can inhibit catalysis in vitro

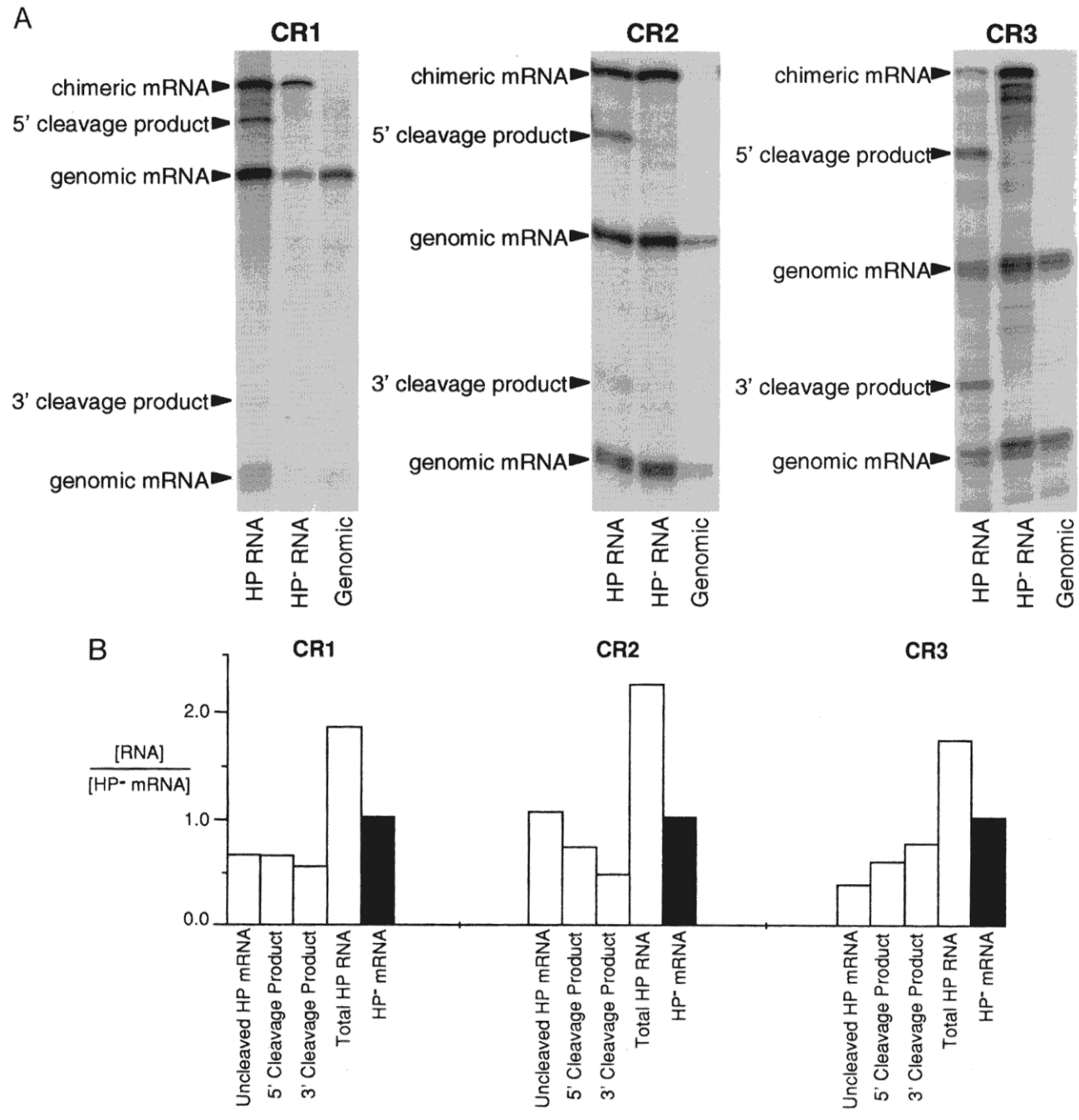

FIGURE 6. Self-cleavage of hairpin ribozymes in the *PGK1* coding region. **A:** Arrows mark fragments corresponding to uncleaved chimeric mRNA, cleavage products, and genomic *PGK1* mRNA sequences detected in yeast carrying chimeric *PGK1* genes with hairpin ribozymes in CR1, CR2, or CR3 sites (Fig. 1B). **B:** Abundance of uncleaved HP mRNA and cleavage products (open) relative to HP^- mRNA (filled) for chimeric mRNAs with hairpin ribozymes located at each site.

(Fedor & Uhlenbeck, 1990; Uhlenbeck, 1995) and might account for limited self-cleavage of ribozymes at CR1 and CR2 sites. However, secondary structure modeling of chimeric RNAs using M-FOLD computations (Zuker, 1994) revealed no differences among HP mRNAs in the tendency of ribozyme insertions to adopt alternate structures.

Cleavage products lacking terminal cap and poly (A) structures are stable

Among the functions attributed to mRNA terminal cap and poly A structures is regulation of mRNA stability. In yeast, mRNA degradation can be initiated either by poly A shortening, by decapping, or by endonucleo-

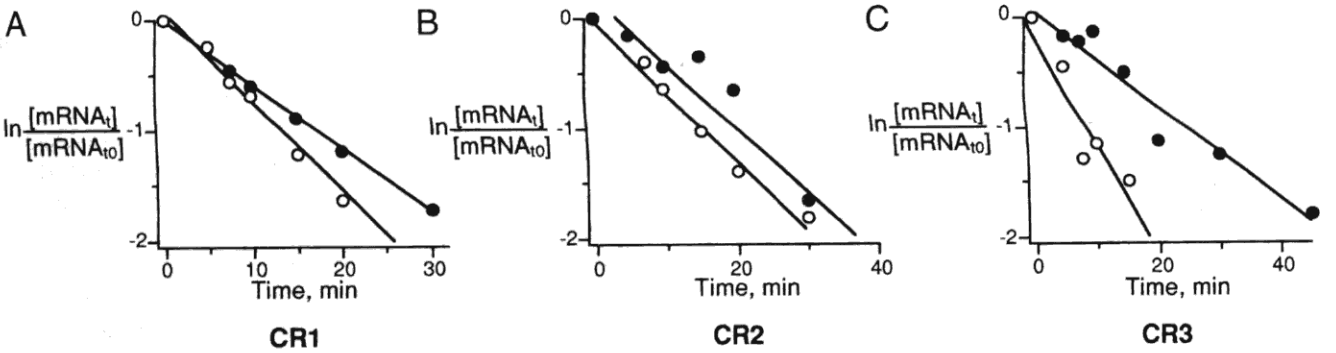

FIGURE 7. Self-cleavage rates of hairpin ribozymes in the coding region. Intracellular decay rates of HP and HP$^-$ mRNAs were measured from the disappearance of intact chimeric mRNA following a burst of transcription. **A:** Intracellular decay rates of chimeric mRNAs with HP (open circle) and HP$^-$ (filled circle) insertions in CR1 were 0.073 min^{-1} and 0.064 min^{-1}, respectively, giving an intracellular self-cleavage rate of 0.010 min^{-1}. **B:** Chimeric mRNAs with HP (open circle) or HP$^-$ (filled circle) insertions in CR2 decayed at a similar rate of 0.06 min^{-1}. **C:** Chimeric mRNAs with HP (open circle) or HP$^-$ (filled circle) insertions in CR3 decayed at rates of 0.091 min^{-1} and 0.040 min^{-1}, respectively, giving an intracellular self-cleavage rate of 0.050 min^{-1}.

lytic cleavage in the body of an mRNA (reviewed in Beelman & Parker, 1995; Jacobson & Peltz, 1996). *PGK1* mRNA, in particular, undergoes deadenylation-dependent 3′ to 5′ decay and decapping-dependent 5′ to 3′ decay (Muhlrad & Parker, 1994; Muhlrad et al., 1995). Self-cleavage of chimeric mRNA offers an opportunity to examine the stability of *PGK1* mRNAs that lack terminal structures because cleavage generates a capped 5′ fragment with no poly (A) and a polyadenylated 3′ fragment with no cap.

Cleavage product concentrations reflect rates of self-cleavage and product degradation. At steady state, product formation and degradation rates are balanced, or:

$$k_{cleavage}\,[\text{HP mRNA}] = k_{degradation}\,[\text{product}].$$

Therefore, product degradation rates can be calculated from $k_{cleavage}$ values and the relative abundance of uncleaved HP mRNA and cleavage products at steady state (Brehm & Cech, 1983). Surprisingly, both 5′ and 3′ cleavage products degrade at rates very similar to degradation rates measured for corresponding HP$^-$ mRNAs despite the loss of terminal caps or poly A (Table 3).

DISCUSSION

What limits intracellular cleavage?

The similarity of hairpin cleavage rates in intracellular and in vitro reactions and the similar effects of $G_{+1}A$ and $G_{21}U$ mutations shows that, in a favorable mRNA sequence context, no fundamental change in the hairpin cleavage mechanism results from the activity of RNA-binding proteins or the intracellular ionic environment.

Modest reductions in intracellular cleavage rates and the effects of a $G_{21}U$ mutation could be explained by a small difference between in vivo and in vitro kinetic mechanisms. In vitro, the reaction equilibrium favors ligation over cleavage when the ribozyme is completely bound by substrate or products (Feldstein & Bruening, 1993; Hegg & Fedor, 1995). For the hairpin sequence examined here, the 3′ cleavage product binds the ribozyme with low affinity and cleavage is driven by rapid product dissociation and dilution under standard in vitro assay conditions. Partitioning of the ribozyme-product complex between ligation and dissociation would shift to favor ligation if the helix formed between the ribozyme and the 3′ cleavage product is

TABLE 3. Intracellular stability of HP mRNA cleavage products

Insertion site	5′ Cleavage product		3′ Cleavage product	
	[Intact mRNA][a] / [Cleavage product]	$k_{degradation}$[b] (per min)	[Intact mRNA][a] / [Cleavage product]	$k_{degradation}$[b] (per min)
UTR	0.32 ± 0.01	0.019	0.72 ± 0.39	0.042
CR1	1.04 ± 0.27	0.022	1.33 ± 0.76	0.028
CR3	0.65 ± 0.17	0.038	0.51 ± 0.10	0.030

[a]Mean and range of values obtained from three or more preparations of yeast RNA at steady state.
[b]Calculated from $k_{degradation} = k_{cleavage}$ ([Intact HP mRNA]/[Cleavage product]) by assuming that $k_{cleavage}$ [Intact HP mRNA] = $k_{degradation}$[Cleavage product] at steady state and using the average of $k_{cleavage}$ values in Table 2, as described in the text.

more stable in vivo. Thus, slower product dissociation in vivo could reduce apparent cleavage rates by allowing product ligation.

If product dissociation is slow enough to limit cleavage rates in vivo but not in vitro, a mutation that slows cleavage without affecting product dissociation would inhibit in vivo cleavage less than in vitro cleavage. Therefore, the twofold difference in the impact of the $G_{21}U$ mutation on in vitro and in vivo cleavage rates also is consistent with a small shift in the balance between ligation and product dissociation. Changes in the stability of RNA helices in vivo could arise from the activity of RNA binding proteins or differences in counterions. Alternatively, the small apparent difference in the effect of the $G_{21}U$ mutation on in vivo and in vitro cleavage kinetics could stem from error in measurements of intracellular cleavage rates.

Differences in self-cleavage among ribozymes located in coding region sites are more apparent than real because they result mostly from variation in the intrinsic degradation rates that modulate the impact of cleavage on mRNA abundance. Translation alone or a structural difference between coding and noncoding regions cannot account for the modest inhibition of self-cleavage of ribozymes in CR1 and CR2 sites because a ribozyme in one coding region site, CR3, cleaves at the same rate as a ribozyme in the untranslated region. Reduced cleavage efficiency in vitro can reflect folding of ribozyme sequences into nonfunctional structures (Fedor & Uhlenbeck, 1990; Uhlenbeck, 1995). If assembly into nonfunctional structures reduces intracellular self-cleavage at CR1 or CR2, the absence of any correlation with in vitro cleavage efficiency indicates that intracellular and in vitro folding pathways differ. Variation in ribosome occupancy also might explain small differences in self-cleavage rates among ribozymes in coding region sites if ribozyme assembly is in kinetic competition with translation.

Intracellular stability of ribozyme cleavage products

Our finding that self-cleavage products remain as stable as uncleaved mRNAs is surprising initially because of the importance of mRNA terminal structures in regulation of mRNA turnover (reviewed in Beelman & Parker, 1995; Jacobson & Peltz, 1996). Cleavage products could resemble uncleaved mRNAs in stability if chimeric mRNAs self-cleave in vitro where products are not subject to degradation. This possibility is excluded, however, by proof that added ribozyme transcripts remain intact throughout RNA isolation and analysis (Figs. 2, 3B,C), by the difference in amounts of 5′ and 3′ cleavage products in vivo (Fig. 3E; Table 3), and by the variation in the proportion of cleaved and uncleaved mRNAs over an intracellular decay time course (Fig. 4B).

An explanation of cleavage product stability could lie in models of mRNA degradation mechanisms that invoke a functional interplay between mRNA translation and degradation mediated through cap and poly (A) structures (Jacobson & Peltz, 1996). If mRNAs degrade during cap and poly (A)-dependent translation, loss of terminal structures might disrupt translation, thereby expelling cleavage products from the degradation pathway. Alternatively, mRNA fragments with 2′,3′-cyclic phosphate and 5′ hydroxyl termini might not be substrates for exonucleolytic degradation because yeast poly (A) nuclease leaves 3′ hydroxyl termini (Lowell et al., 1992) and decapping leaves 5′ phosphates (Stevens, 1980).

If loss of terminal structures rescues cleavage products from degradation, however, product stability would increase and not stay the same. More likely, ribozyme-mediated cleavage simply does not short circuit the normal degradation pathway. mRNA fragments would decay at the same rate as intact mRNAs if the RNA–protein complex that ushers mRNAs through the degradation pathway remains functionally intact despite the loss of one phosphodiester.

Implications for gene inactivation by antisense ribozymes

The effects of cleavage on mRNA abundance have clear implications for antisense ribozyme applications. The relationship among intrinsic decay and self-cleavage rates and steady-state RNA levels demonstrates how the stability of an mRNA affects its suitability as an antisense target. Although intracellular cleavage is three times faster than normal *PGK1* mRNA turnover, cleavage reduces chimeric mRNA levels only fourfold. A more labile mRNA target, such as c-*myc*, with an intrinsic turnover rate nearly equal to the intracellular cleavage rate (Wisdom & Lee, 1991), would be reduced only twofold. In contrast, the oncogenic counterpart of c-*myc*, expressed as an immunoglobulin fusion mRNA in B cells of patients with Burkitt's lymphoma, is three- to eightfold more stable than its unmodified counterpart (Eick et al., 1985) and would be reduced four- to ninefold by cleavage at the same rate.

Because antisense ribozymes can eliminate target RNAs only when cleavage is much faster than normal degradation, the impact of antisense ribozyme-mediated cleavage will be greatest with stable RNA targets. Because an inhibitory mutation affects in vitro and in vivo cleavage similarly, ribozyme modifications that accelerate cleavage in vitro will likely accelerate intracellular cleavage as well. Faster ribozymes should extend the range of feasible antisense targets to include less stable RNAs. Model systems used for antisense ribozyme screening will have greater predictive value for gene inactivation when model targets and intended targets share the same intrinsic stability. Furthermore,

genes regulated by changes in mRNA stability will vary accordingly in susceptibility to ribozyme-mediated inactivation, an important consideration in the use of antisense ribozymes to probe gene function.

mRNA cleavage, particularly in coding sequences, almost certainly destroys translatability. However, stable mRNA fragments might continue to function in viral packaging, for example, or provide binding sites for regulatory proteins. In view of the potential for RNA recombination, the persistence of cleavage products is a concern in antiviral ribozyme applications.

Intracellular self-cleavage rates define the maximum activity expected for a fully assembled complex between a ribozyme and a separate RNA target. Thus, self-cleavage rates provide a gauge to indicate when slow transport or binding steps limit ribozyme-mediated cleavage of separate RNA targets.

MATERIALS AND METHODS

Plasmid construction and propagation

Plasmids were constructed using conventional methods (Sambrook et al., 1989). Synthetic DNA cassettes with HP and HP$^-$ sequences were inserted into the unique *Cla* I site in the 3′ untranslated region (UTR) of *PGK1* as a the *Bam*H I–*Hin*d III fragment in pRS316 (Sikorski & Hieter, 1989), kindly provided by Stu Peltz and Allan Jacobson. Ribozyme cassettes were PCR amplified for insertion into the unique *Kpn* I site of *PGK1* (CR1) using 5′-GCACCTGGTACCATACAAACAG AGAAGTCAACC-3′ and either 5′-GACCGTGGTACCATA AACAGGACTGTCATCTAG-3′ or 5′-GACCGTGGTACCAT AAACAGGATTGTCATCTAG-3′ as HP or HP$^-$ primers, respectively. A linker with the *Cla* I-compatible *Nar* I site, 5′-TAACGGCGCC-3′, was first inserted into the unique *Msc* I site of *PGK1* (CR2), followed by insertion of the HP or HP$^-$ cassette. Primers 5′-GCAGTCGGATCCCGATACAAACAG AGAAGTCAACC-3′ and either 5′-CTCAGGGGATCCGATA AACAGGACTGTCATCTAG-3′ or 5′-CTCAGGGGATCCGA TAAACAGGATTGTCATCTAG-3′ were used to amplify HP or HP$^-$ cassettes, respectively, digested with *Bam*H I, and inserted into the unique *Bgl* II site of *PGK1* (CR3).

The HP$^{G_{21}U}$ ribozyme insertion was created through mutagenic PCR (Chen & Przybyla, 1994). First, *PGK1* sequences with or without *PGK1* regulatory sequences were amplified between the *Bam*H I site and the HP insertion from a pGEM-3Zf(−) (Promega) construct using a primer corresponding to the T7 promoter, 5′-TAATACGACTCACTATAG-3′, and a primer encoding the $G_{21}U$ mutation, 5′-ACGTGTGTTTATCT GGTTGAC-3′. The PCR product was combined with a primer derived from adjacent *PGK1* and pGEM-3Zf(−) sequences, 5′-GGTGACACTATAGAATACTCAAG-3′, and used to amplify the remainder of *PGK1* and vector sequences and then transferred as a *Bam*H I–*Hin*d III fragment into pRS316.

Fusion of chimeric *PGK1* genes to the GAL1-10 regulatory region began with PCR amplification of a 270-base pair GAL1-10 fragment from pTGU-URA (Fedor et al., 1988) using primers 5′-GGACGGAATCTAGAGAGCCCCATTATCTTA GCC-3′ and 5′-CGGTCGAATCTAGAGGGGCCAGGTTACT GCC-3′, which was then ligated into the *Xba* I site of pRS316. *PGK1* regulatory sequences located more than 251 base pairs upstream of the RNA start site were deleted from chimeric genes in pGEM-3Zf(−) vectors by PCR amplification with primers 5′-CGCGGATCCGATCGTACTGTTACTCTCTCT-3′ and 5′-GGTGACACTATAGAATACTCAAG-3′, digestion with *Bam*H I and *Hin*d III, and insertion into the pRS316 vector bearing the GAL1-10 sequence.

Templates for in vitro transcription of RNAs for self-cleavage assays and hybridization probes for ribozymes in CR1 were prepared using 5′-GCACCTGGATCCTCGGTCCA GAAGTTGAAG-3′ and 5′-GACCGTGGATCCTTCCAACAA GAAACCGGC-3′ to prime amplification of a 356-base pair fragment spanning the CR1 insertion site that was digested with *Bam*H I and inserted into pGEM-4Z in the antisense orientation relative to the T7 promoter and linearized by digestion with *Nde* I for transcription of hybridization probes. Insertions in the sense orientation were linearized with *Eco*R I for transcription of in vitro cleavage substrates.

Kpn I–*Sal* I fragments spanning HP and HP$^-$ sequences at CR2 were inserted into pGEM-4Z, and linearized by digestion with *Nde* I for transcription of hybridization probes, or inserted into pGEM-3Zf(−) and linearized by digestion with *Sal* I for transcription of in vitro cleavage substrates.

Xba I–*Sna*B I fragments spanning the UTR insertion site were inserted into pGEM-4Z that had been digested with *Hin*d III, filled in with Klenow fragment, and then digested with *Xba* I, and templates for transcription of hybridization probes were linearized with *Bgl* II. *Bgl* II–*Hin*d III fragments spanning HP and HP$^-$ sequences in the UTR site were inserted into pGEM-3Zf(−) and templates for transcription of in vitro cleavage substrates were linearized by digestion with *Ssp* I. A *Bgl* II–*Ssp* I fragment spanning the HP$^{G_{21}U}$ sequence in the UTR site was ligated into *Bam*H I and *Hinc* II-digested pGEM-4Z and linearized with *Nde* I for transcription of hybridization probes or ligated into *Bam*H I and *Hinc* II-digested pGEM-3Zf(−) and linearized with *Hin*d III for transcription of in vitro cleavage substrates.

Templates for transcription of CR3 hybridization probes were prepared using 5′-GCACCTGGATCCGAAAAGTTC GCTGCTGGT-3′ and 5′-GACCGTGGATCCCGGATAAGAA AGCAACAC-3′ to prime amplification of a 297-base pair fragment spanning the CR3 insertion site that was digested with *Bam*H I and inserted into pGEM-4Z in the antisense orientation relative to the T7 promoter and linearized by digestion with *Nde* I.

A *Cla* I–*Kpn* I fragment of the yeast ACT1 gene (kindly provided by Allan Jacobson) was inserted into *Acc* I–*Kpn* I-digested pGEM-3Zf(−) and linearized with *Hin*d III for transcription of hybridization probes.

pGEM and pRS316 derivatives were propagated in *Escherichia coli* strains TG-1 (Sambrook et al., 1989), JM109 (Yanisch-Perron, 1985), or MV1190 [supE, thi, Δ(lac-proAB), Δ(srl-recA)306::TN10, [F′, proAB$^+$, lacI^q, lacZΔM15], a generous gift of M. Volkert. pRS316 derivatives were propagated in *Saccharomyces cerevisiae* strain N218 (mat a, ura3-52, rpb1-1, his3 Δ200) carrying a temperature-sensitive allele of the β subunit of RNA polymerase II (Nonet et al., 1987).

Preparation and quantitation of RNAs

RNA was extracted from yeast using a 50 mM $NaCO_2CH_3$, 10 mM EDTA, 1% SDS, pH 5.0, buffer and phenol at 68 °C as described (Köhrer & Domdey, 1991) except that yeast were

frozen in a dry ice/ethanol bath immediately after pelleting and RNA was stored in 10 mM $NaCO_2CH_3$, 1 mM EDTA, pH 5, at −20 °C or at 4 °C when in use. Yeast RNA also was extracted in LiCl buffer (Kaiser et al., 1994) for control experiments.

^{32}P-labeled RNAs were prepared by T7 RNA polymerase transcription of linearized plasmids, as described (Milligan & Uhlenbeck, 1989), in 10-μL reactions with 300 ng template, 0.1 mg/mL T7 RNA polymerase, 40 μCi [α-^{32}P] ATP or [α-^{32}P] CTP with the corresponding nucleotide triphosphate at a concentration of 0.2 mM and 2.0 mM each of the remaining three nucleotides at pH 7.5 for 30 min at 37 °C. For transcription of unlabeled RNAs, nucleotide triphosphate and $MgCl_2$ concentrations were increased to 4 mM and 27 mM, respectively. Transcripts were fractionated on denaturing gels and eluted into 100 mM $NaCO_2CH_3$, 10 mM EDTA, pH 5, at 4 °C. The fraction that remained uncleaved after transcription was kept intact by storage in 10 mM $NaCO_2CH_3$, 1 mM EDTA, pH 5. ^{32}P RNA concentrations were determined from specific activities. Unlabeled RNA concentrations were calculated from absorbance at 260 nm assuming a residue extinction coefficient of 6.6×10^3 M^{-1} cm^{-1}.

Yeast RNAs were identified and quantitated using hybridization-RNase protection assays as described (Sambrook et al., 1989) with 10 μg yeast RNA and 75,000 CPM ^{32}P-labeled probe in each reaction. After hybridization for 12–16 h at 45 °C and digestion with 40 μg/mL RNase A and 2 μg/mL RNase T_1 at 25 °C for 30 min, protected fragments were fractionated on denaturing gels and quantitated by radioanalytic scanning (Molecular Dynamics). In control experiments with in vitro transcripts, hybridization reactions contained 0.1 ng transcript and 10 μg carrier tRNA was added during RNase digestion.

Two fragments corresponding to genomic mRNA sequences upstream and downstream of the hairpin insertion site appeared in equal amounts, confirming that large and small fragments are detected with the same sensitivity. Radioactive signal increased proportionately when yeast RNA was increased from 10 to 40 μg, confirming linearity. Yeast RNA concentrations were normalized to the amount of genomic *PGK1* mRNA in yeast grown in glucose or to *ACT1* mRNA in yeast grown in galactose. Reported mRNA levels are the average of 3–10 experiments.

Kinetic analysis in vitro

Self-cleavage kinetics were measured in vitro using uncleaved chimeric RNAs that were fractionated from in vitro transcription reactions on denaturing gels. ^{32}P RNA was diluted into 5 mM $NaCO_2CH_3$, 0.1 mM EDTA, pH 5, to 30 pM, incubated at 70 °C for 2 min, then equilibrated at 24 °C. Reactions were initiated by threefold dilution into 50 mM Tris-Cl, 10 mM $MgCl_2$, 0.1 mM EDTA, pH 7.5, at 24 °C. Samples were removed at intervals, quenched by threefold dilution into 8 M urea, 25 mM EDTA, 0.002% xylene cyanole, 0.002% bromophenol blue, and fractionated on denaturing gels. Cleavage rates varied less than 3.0% among multiple experiments.

Kinetic analysis in vivo

mRNA decay rates were determined as described (Parker et al., 1991). Yeasts were grown to an absorbance of 0.2 at 600 nm at 24 °C in minimal medium (0.67% yeast nitrogen base without amino acids) with L-histidine (20 mg/L), leucine (30 mg/L), and 2% raffinose. Yeasts were pelleted, resuspended in 1/10 volume of minimal medium but with 4% galactose, and incubated at 24 °C for 2 h, then pelleted and resuspended in minimal medium with 4% glucose to prevent further transcription at the start of the decay time course. Samples were collected at intervals and RNA was extracted and quantitated using hybridization-RNase protection assays as described above.

ACKNOWLEDGMENTS

We are very grateful to Stu Peltz and Allan Jacobson for advice and generous gifts of strains and plasmids, to Olke Uhlenbeck for helpful discussions, and to Reid Gilmore, Michael Green, Bob Lahue, Michael Rosbash, Jamie Williamson, and Phil Zamore for comments on the manuscript. This work was supported by NIH grant GM46422.

Received March 28, 1997; returned for revision April 14, 1997; revised manuscript received June 4, 1997

REFERENCES

Beelman CA, Parker R. 1995. Degradation of mRNA in eukaryotes. *Cell 81*:179–183.

Bertrand EL, Rossi JJ. 1994. Facilitation of hammerhead ribozyme catalysis by the nucleocapsid protein of HIV-1 and the heterogeneous nuclear ribonucleoprotein A1. *EMBO J 13*:2904–2912.

Brehm SL, Cech TR. 1983. Fate of an intervening sequence ribonucleic acid: Excision and cyclization of the *Tetrahymena* ribosomal ribonucleic acid intervening sequence in vivo. *Biochemistry 22*:2390–2397.

Burke JM, Butcher SE, Sargueil B. 1996. Structural analysis and modifications of the hairpin ribozyme. *Nucleic Acids Mol Biol 10*:129–143.

Buzayan JM, Gerlach WL, Bruening G. 1986. Nonenzymatic cleavage and ligation of RNAs complementary to a plant virus satellite RNA. *Nature 323*:349–353.

Celander DW, Cech TR. 1991. Visualizing the higher order folding of a catalytic RNA molecule. *Science 251*:401–407.

Chen B, Przybyla AE. 1994. An efficient site-directed mutagenesis method based on PCR. *BioTechniques 17*:657–659.

Chowrira BM, Berzal-Herranz A, Burke J. 1991. Novel guanosine requirement for catalysis by the hairpin ribozyme. *Nature 354*:320–322.

Chowrira BM, Berzal-Herranz A, Burke JM. 1993. Ionic requirements for RNA binding, cleavage, and ligation by the hairpin ribozyme. *Biochemistry 32*:1088–1095.

Coetzee T, Herschlag D, Belfort M. 1994. *E. coli* proteins, including the ribosomal protein S12, facilitate in vitro splicing of phage T4 introns by acting as RNA chaperones. *Genes & Dev 8*:1575–1588.

Crisell P, Thompson S, James W. 1993. Inhibition of HIV-1 replication by ribozymes that show poor activity in vitro. *Nucleic Acids Res 21*:5251–5255.

Eick D, Piechaczyk M, Henglein B, Blanchard JM, Traub B, Kofler E, Wiest S, Lenoir GM, Bornkamm GW. 1985. Aberrant c-myc RNAs of Burkitt's lymphoma cells have longer half-lives. *EMBO J 4*:3717–3725.

Fedor MJ, Lue NF, Kornberg RD. 1988. Statistical positioning of nucleosomes by specific protein-binding to an upstream activating sequence in yeast. *J Mol Biol 204*:109–127.

Fedor MJ, Uhlenbeck OC. 1990. Substrate sequence effects on "hammerhead" RNA catalytic efficiency. *Proc Natl Acad Sci USA 87*:1668–1672.

Feldstein PA, Bruening G. 1993. Catalytically active geometry in the reversible circularization of "mini-monomer" RNAs derived from

the complementary strand of tobacco ringspot virus satellite RNA. *Nucleic Acids Res 21*:1991–1998.
Feldstein PA, Buzayan JM, Bruening G. 1989. Two sequences participating in the autocatalytic processing of satellite tobacco ringspot virus complementary RNA. *Gene 82*:53–61.
Grosshans CA, Cech TR. 1989. Metal ion requirements for sequence-specific endoribonuclease activity of the *Tetrahymena* ribozyme. *Biochemistry 28*:6888–6894.
Hampel A, Tritz R. 1989. RNA catalytic properties of the minimum (−)sTRSV sequence. *Biochemistry 28*:4929–4933.
Hegg LA, Fedor MJ. 1995. Kinetics and thermodynamics of intermolecular catalysis by hairpin ribozymes. *Biochemistry 34*:15813–15828.
Herrick D, Parker R, Jacobson A. 1990. Identification and comparison of stable and unstable mRNAs in *Saccharomyces cerevisiae*. *Mol Cell Biol 10*:2269–2284.
Homann M, Tabler M, Tzortzakaki S, Sczakiel G. 1994. Extension of helix II of an HIV-1-directed hammerhead ribozyme with long antisense flanks does not alter kinetic parameters in vitro but causes loss of the inhibitory potential in living cells. *Nucleic Acids Res 22*:351–357.
Jacobson A, Peltz SW. 1996. Interrelationships of the pathways of mRNA decay and translation in eukaryotic cells. *Annu Rev Biochem 65*:693–739.
Kaiser C, Michaelis S, Mitchell A. 1994. *Methods in yeast genetics*. New York: Cold Spring Harbor Laboratory Press. pp 151–152.
Keese P, Symons RH. 1987. The structure of viroids and virusoids. In: Semancik JS, ed. *Viroids and viroid-like pathogens*. Boca Raton: CRC Press. pp 1–47.
Köhrer KB, Domdey H. 1991. Preparation of high molecular weight RNA. *Methods Enzymol 194*:398–405.
Long DM, Uhlenbeck OC. 1993. Self-cleaving RNA. *FASEB J 7*:25–30.
Lowell JE, Rudner DZ, Sachs A. 1992. 3′-UTR-dependent deadenylation by the yeast poly(A) nuclease. *Genes & Dev 6*:2088–2099.
Madhani HD, Guthrie C. 1992. A novel base-pairing interaction between U2 and U6 snRNA suggests a mechanism for the catalytic activation of the spliceosome. *Cell 71*:803–817.
Milligan JF, Uhlenbeck OC. 1989. Synthesis of small RNAs using T7 RNA polymerase. *Methods Enzymol 180*:51–62.
Mohr G, Zhang A, Gianelos JA, Belfort M, Lambowitz AM. 1992. The *Neurospora* CYT-18 protein suppresses defects in the phage T4 *td* intron by stabilizing the catalytically active structure of the intron core. *Cell 69*:483–494.
Muhlrad D, Decker CJ, Parker R. 1995. Turnover mechanisms of the stable yeast *PGK1* mRNA. *Mol Cell Biol 15*:2145–2156.
Muhlrad D, Parker R. 1994. Premature translational termination triggers mRNA decapping. *Nature 370*:578–581.
Noller HF, Hoffarth V, Zimniak L. 1992. Unusual resistance of peptidyl transferase to protein extraction procedures. *Science 256*:1416–1418.
Nonet M, Scafe S, Sexton J, Young R. 1987. Eucaryotic RNA polymerase conditional mutant that rapidly ceases mRNA synthesis. *Mol Cell Biol 7*:1602–1611.
Pan T. 1995. Higher order folding and domain analysis of the ribozyme from *Bacillus subtilis* ribonuclease P. *Biochemistry 34*:902–909.
Pan T, Long DM, Uhlenbeck OC. 1993. Divalent metal ions in RNA folding and catalysis. In: Gesteland RF, Atkins JF, eds. *The RNA world*. New York: Cold Spring Harbor Laboratory Press. pp 271–302.
Parker R, Herrick D, Peltz SW, Jacobson A. 1991. Measurement of mRNA decay rates in *Saccharomyces cerevisiae*. *Methods Enzymol 194*:415–423.
Peltz SW, Jacobson A. 1993. mRNA turnover in *Saccharomyces cerevisiae*. In: Brawerman G, Belasco J, eds. *Control of mRNA stability*. New York: Academic Press. pp 291–328.
Piccirilli JA, Vyle JS, Caruthers MH, Cech TR. 1993. Metal ion catalysis by the *Tetrahymena* ribozyme. *Nature 361*:85–88.
Sambrook J, Fritsch EF, Maniatis T. 1989. *Molecular cloning: A laboratory manual*. New York: Cold Spring Harbor Laboratory Press.
Sikorski RS, Hieter P. 1989. A system of shuttle vectors and yeast host strains designed for efficient manipulation of DNA in *Saccharomyces cerevisiae*. *Genetics 122*:19–27.
Smith D, Burgin AB, Haas ES, Pace N. 1992. Influence of metal ions on the ribonuclease P reaction. Distinguishing substrate binding from catalysis. *J Biol Chem 267*:2429–2436.
Stevens A. 1980. Purification and characterization of a *Saccharomyces cerevisiae* exoribonuclease which yields 5′-mononucleotides by a 5′ to 3′ mode of hydrolysis. *J Biol Chem 255*:3080–3085.
Symons RH. 1992. Small catalytic RNAs. *Annu Rev Biochem 61*:641–671.
Tsuchihashi Z, Koshla M, Herschlag D. 1993. Protein enhancement of hammerhead ribozyme catalysis. *Science 262*:99–102.
Uhlenbeck OC. 1995. Keeping RNA happy. *RNA 1*:4–6.
Weeks KM, Cech TR. 1995. Protein facilitation of group I splicing by assembly of the catalytic core and the 5′ splice site domain. *Cell 82*:221–230.
Welch PJ, Hampel A, Barber J, Wong-Staal F, Yu M. 1996. Inhibition of HIV replication by the hairpin ribozyme. *Nucleic Acids and Mol Biol 10*:314–327.
Wisdom R, Lee W. 1991. The protein-coding region of c-myc mRNA contains a sequence that specifies rapid mRNA turnover and induction by protein synthesis inhibitors. *Genes & Dev 5*:232–243.
Yanisch-Perron C. 1985. Improved M13 phage cloning vectors and host strains: Nucleotide sequences of the M13mp18 and pUC19 vectors. *Gene 33*:103–119.
Zarrinkar PP, Williamson JR. 1994. Kinetic intermediates in RNA. *Science 265*:918–924.
Zhang F, Ramsay ES, Woodson SA. 1995. In vivo facilitation of *Tetrahymena* group I intron splicing in *Escherichia coli* pre-ribosomal RNA. *RNA 3*:284–292.
Zuker M. 1994. Prediction of RNA secondary structure by energy minimization. *Methods Mol Biol 25*:267–294.